# Selective sulfur removal from semi-dry flue gas desulfurization

# coal fly ash for concrete and carbon dioxide capture applications

- 3 Raghavendra Ragipani<sup>a</sup>, Eleanor Escobar<sup>a</sup>, Dale Prentice<sup>b,c</sup>, Steven
- 4 Bustillos<sup>b,d</sup>, Dante Simonetti<sup>c,d,e</sup>, Gaurav Sant<sup>b,c,e,f</sup>, Bu Wang<sup>a</sup>\*
- 5 <sup>a</sup> Department of Civil and Environmental Engineering, University of Wisconsin-Madison, Madison,
- 6 Wisconsin, United States

1

2

- 7 bLaboratory for the Chemistry of Construction Materials (LC2), Department of Civil and Environmental
- 8 Engineering, University of California, Los Angeles, Los Angeles, California, 90095, United States
- 9 <sup>c</sup> Institute for Carbon Management (ICM), University of California, Los Angeles, Los Angeles, California
- 10 90095, United States
- 11 d Department of Chemical and Biomolecular Engineering, University of California, Los Angeles, Los
- 12 Angeles, California 90095, United States
- 13 <sup>e</sup> California Nanosystems Institute, University of California, Los Angeles, Los Angeles, California 90095,
- 14 United States
- 15 Department of Materials Science and Engineering, University of California, Los Angeles, Los Angeles,
- 16 California 90095, United States
- \*\*Corresponding author: bu.wang@wisc.edu

## **Abstract**

- 19 High-sulfur mixed fly ash residues from semi-dry flue gas desulfurization units in coal-
- 20 fired power plants are unsuitable for use as supplementary cementitious material (SCM) for
- 21 concrete production or carbon dioxide utilization. In this work, we explore the potential for
- 22 upcycling a representative spray dry absorber ash (10.44 wt.% SO<sub>3</sub>) into concrete-SCM by

selective sulfur removal via weak acid dissolution while simultaneously exploring the possibility for CO<sub>2</sub> capture. Towards this effort, parametric studies varying liquid-to-solid ratio, acidity, and CO<sub>2</sub> pressure were conducted in a batch reactor to establish the sulfur removal characteristics in de-ionized water, nitric acid, and carbonic acid, respectively. The dissolution studies show that the leaching of sulfur from calcium sulfite hemihydrate, which is the predominant S phase, is rapid and achieves a concentration plateau within 5 minutes, and subsequently, appears to be controlled by the primary mineral solubility. Preferential S removal was sufficient to meet SCM standards (e.g., 5.0 wt% as per ASTM C618) using all three washing solutions with 0.62-0.72 selectivity ( $\hat{S}$ ), defined as the molar ratio of S to Ca in the leachate, for a raw fly ash with bulk  $\hat{S}$  = 0.3. Acid dissolution with 1.43 meq/g of ash or under 5 atm CO<sub>2</sub> retained >18 wt.% CaO and other Si-, Al-rich phases in the fly ash. Based on the experimental findings, two sulfur removal schemes were suggested for either integration with CO<sub>2</sub> capture and utilization processes using flue gas or to produce fly ash for use as a SCM.

Keywords: washing, supplementary cementitious material, calcium sulfite, gypsum, spray dry

## 1 Introduction

absorber, fly ash

Utilization of fly ash from coal combustion power plants as a feedstock for carbon dioxide (CO<sub>2</sub>) mineralization processes has been a subject of investigation in recent years (Bobicki et al., 2012; Pan, 2012; Wee, 2013). The most common route among the CO<sub>2</sub> mineralization processes is based on aqueous carbonation, wherein ions such as Ca<sup>2+</sup> extracted from solid feedstocks by an aqueous medium react with CO<sub>2</sub> to precipitate sparingly soluble carbonates (Lackner et al., 1995; Olajire, 2013). Fly ash is considered an ideal feedstock for such processes because it is alkaline in nature, rich in calcium and reactive. The fine particle size and co-production with

46 CO<sub>2</sub> at power plants minimize the need for pretreatment (i.e., grinding) and transportation costs 47 (Wee, 2013). Furthermore, these CO<sub>2</sub> mineralization processes can be modified to produce 48 valuable products, such as precipitated calcium carbonate (Chang et al., 2017; Eloneva et al., 49 2012; Teir et al., 2005), rare earth elements (Vaziri Hassas et al., 2020), and concrete (Lim et al., 50 2010; Mehdipour et al., 2019; Wei et al., 2018), providing attractive routes for CO<sub>2</sub> capture and 51 utilization. 52 Fly ash conforming to ASTM C618 standard (i.e., Class C and F fly ash) has often been 53 utilized as a supplementary cementitious material (SCM) for concrete production (ASTM 54 Standard C618 – 19, 2010). Recycling fly ash to replace Portland cement provides significant 55 environmental and technical benefits (Samad and Shah, 2017). Thus, it is desirable for CO<sub>2</sub> 56 mineralization processes to utilize alternative fly ash streams, i.e., those not in compliance with 57 ASTM C618, as a feedstock. A common type of non-compliant fly ash (with SO<sub>3</sub> wt% >5.0 as 58 per ASTM C618) is that contains semi-dry and dry flue gas desulfurization (FGD) impurities 59 (e.g., S-bearing compounds), which increased substantially after enforcement of the Mercury and 60 Air Toxics (MATS) rule in the United States in 2015 (DeVilbiss and Ray, 2017). Coal-fired 61 power plants have preferred dry and semi-dry scrubbing FGD systems, especially for retrofitting 62 power plants, owing to their low installation cost and decreased water consumption compared to 63 wet systems (Carpenter, 2012; Hoff and DeVilbiss, 2016). However, a vast majority of dry 64 scrubbing FGD ashes (~80%) are disposed into ash ponds or landfills, with only 20% being 65 recycled into mine reclamation and soil conditioning applications (Cruz et al., 2017; Ladwig and Blythe, 2017). In addition to the increasing costs of ash storage and landfilling, contamination of 66 67 surface waters due to the leaking of ash ponds presents an environmental concern (Harkness et 68 al., 2016).

In the United States, the most common semi-dry FGD systems are based on spray dry absorber (SDA) technology commissioned upstream to the particulate matter collection filters. As such, these power plants produce mixed residues of FGD products and fly ash (Carpenter, 2012; Sharifi et al., 2019). High sulfur content in these residues is the primary reason for underutilization vis-à-vis fly ashes collected upstream to FGD. The primary sulfur-rich phase in the SDA ashes is calcium sulfite hemihydrate (CaSO<sub>3</sub>.0.5H<sub>2</sub>O), where sulfur is present in the S(IV) oxidation state (Zaremba et al., 2008). In oxygenated aqueous environments, sulfite ions gradually oxidize to sulfate (Fuller and Crist, 1941), which can react with calcium aluminates to form expansive sulfoaluminate ("ettringite"). When used in concrete, these reactions are expected to occur over time, and long-term durability issues arise due to the slow-releasing sulfate (Ríos et al., 2020; Sharifi et al., 2019). This problem is expected to continue to limit the use of SDA ashes for concrete production. Therefore, it is necessary to identify routes for large-scale beneficiation of SDA ashes.

Generally, it is known that the sulfur-rich mineral phases accumulate on the surface of the fly ash, and the grain size of these phases are expected to be smaller than those phases associated with fly ash (Enders, 1996; Izquierdo and Querol, 2012). Thus, the rapid dissolution of the sulfite phase in aqueous solution is expected to control the release of Ca, S, and leachate pH, as shown by previous ash dissolution studies (Izquierdo and Querol, 2012). As such, while it is desirable to utilize SDA ashes for CO<sub>2</sub> mineralization, the rapid release of sulfur under conditions relevant to aqueous carbonation processes could become problematic to directly produce either carbonate minerals or concrete. Sulfur contamination (in the form of sulfite or sulfate) would pose issues associated with purity and durability, respectively, in the two applications.

However, rapid S-release offers promise for pretreatment of SDA ash for selective sulfurremoval. Furthermore, in the event of sulfite phases controlling the calcium solubility and leachate pH, a simultaneous enhancement in sulfite solubility and carbon dioxide absorption capacity is possible due to pH buffering in the pH range of 5–8 as a consequence of sulfitebisulfite equilibrium,  $CO_2(g) + SO_3^{-2} + H_2O \leftrightarrow HCO_3^{-} + HSO_3^{-}$  (Ebrahimi et al., 2003). Understanding leaching characteristics, especially the extraction kinetics, selectivity, and solubility of sulfur from SDA ash vis-à-vis other phases, can enable the development of a process to produce a low-sulfur ash residue. Therefore, herein, we developed a new process to selectively extract and recycle the sulfur content from SDA ash using carbonic acid, which offers the potential for simultaneous CO<sub>2</sub> capture from flue gas. With slight modifications, this process can also be used to produce low-sulfur ash that is compliant with ASTM C618. Since dissolution processes could be water-intensive, a critical study on the process water demand for the proposed scheme with integrated carbon capture was carried out. We comment on process viability based on a comparison of process water circulation rates and losses with that of a commercial wet FGD technology.

### 2 Materials and Methods

#### 2.1 Characterization

91

92

93

94

95

96

97

98

99

100

101

102

103

104

105

106

107

108

109

110

111

112

113

Sulfur-rich fly ash (referred to as W4-SDA in this article) was provided by Weston Power Plant, WI, United States. The ash was generated from a spray dry absorber (SDA; B&W/GEA Niro SDA technology), which was commissioned upstream to the pulse-jet-cleaned fabric filter, thereby collecting a mixed residue of fly ash and FGD products (POWER, 2008). The FGD products from a hydrated lime spray dryer absorber mainly include calcium sulfite(IV) hemihydrate along with minor quantities of calcium sulfate(VI) and unreacted calcium hydroxide

(Carpenter, 2012; Ladwig and Blythe, 2017). In SDA, if fly ash is not precollected, an "off-spec" mixed residue of fly ash (~72%) and FGD products is obtained (Ladwig and Blythe, 2017). Typical Ca-rich class C fly ash from coal power plant is made up of quartz, tricalcium aluminate, aluminosilicates, iron oxide, magnesium oxide etc. Sulfur in typical fly ash is mainly present as anhydrite or sodium sulfate in high-sodium ashes (McCarthy et al., 1990). The raw ash was characterized using an X-ray fluorescence (XRF) spectrometer, and an X-ray diffractometer (XRD; Bruker D8 Discover with Cu-Kα X-ray source) for elemental and mineral phase compositions, respectively.

## 2.2 Dissolution studies

Three sets of dissolution experiments were conducted. These include 1) batch dissolution of ash in DI water at atmospheric conditions, 2) titration of ash slurry using nitric acid, and 3) batch dissolution experiments in a pressurized reactor under 1–5 atm of 100% CO<sub>2</sub>. A typical batch dissolution experiment at atmospheric conditions involved charging of 0.1–4.0 g of SDA ash (measured to the accuracy of 0.001 g) into a 250 cm<sup>3</sup> glass bottle containing de-ionized water (100 or 200 cm<sup>3</sup> with conductivity of <1  $\mu$ S cm<sup>-1</sup> and measured to the accuracy of 0.5%) and stirred at 400±20 rpm on a hot-plate magnetic stirrer. The liquid-to-solid (L/S) ratio was varied in the range of 25–2000 cm<sup>3</sup>g<sup>-1</sup>. The reaction temperature was maintained at 23±2 °C.

Slurry pH was measured using the Orion Ross glass electrode and Thermo Scientific Orion Star pH meter that was regularly calibrated with pH 4.01 and pH 10.01 buffers (slope within 99–100%). Each experiment was repeated at least twice, with at least one experiment without the pH probe to avoid KCl contamination due to pH electrode and accurately measure K concentration in the leachate. Experiments under carbon dioxide (1–5 atm) exposure were conducted in a 50 cm³ benchtop Parr reactor. For each batch experiment, 25 cm³ of de-ionized water was first

added to the reactor, and then ash was added to achieve a slurry with L/S between 25–100 cm<sup>3</sup> g<sup>-1</sup>. The slurry was homogenized via stirring for 30 s. CO<sub>2</sub> was introduced to the reactor (without stirring) via cycles in which the reactor was placed under vacuum and then refilled with 100 % CO<sub>2</sub>. After three of these cycles, the reactor was pressurized with CO<sub>2</sub> to the desired pressure. Subsequently, dissolution was started by stirring the slurry at 800±10 rpm. A liquid sample was collected at the end of the reaction, after the depressurization of the reactor.

Acid titration of the ash slurry was carried out using a Hanna 901C auto-titrator with standardized 1.0 M nitric acid as the titrant, and an initial liquid-to-solid ratio of 25 cm<sup>3</sup> g<sup>-1</sup>. A linear dosing titration was carried out with 0.05 cm<sup>3</sup> doses every 5 seconds until the slurry pH reached 3.0. Intermittent liquid sampling was carried out for analysis. During each batch experiment and titration study, the liquid sample was collected by filtering the slurry using a 0.2 µm syringe filter. An in-sample oxidation procedure of leachate was necessary to oxidize sulfite to sulfate and consequently avoid the formation of sulfur dioxide upon acidification to a pH\le2 for inductively-coupled-plasma optical emission spectrometry (ICP-OES; Varian Vista-MPX, Varian, Palo Alto, CA, USA) analysis. Without oxidation, a positive error in concentration measurement with significant variance was noticed, possibly due to higher nebulization of volatile dissolved gases (SO<sub>2</sub>) into the ICP-OES chamber (Sarudi et al., 2001) (see Appendix A.1 provided as e-component along with the manuscript for measurements using sodium sulfite solution). The in-sample oxidation procedure involved the addition of 0.03 wt.% H<sub>2</sub>O<sub>2</sub> with 1.0 mM HNO<sub>3</sub> to the collected liquid samples in a 1:1 volume ratio. Partial acidification was necessary for instantaneous oxidation. Subsequently, the oxidized sample was diluted and acidified using 0.5 M HNO<sub>3</sub> to match the ICP standard matrix used in this study. Elemental concentrations (Ca, Fe, Mg, Al, Si, S, Na, and K) in the leachate were measured using ICP-OES

137

138

139

140

141

142

143

144

145

146

147

148

149

150

151

152

153

154

155

156

157

158

after calibrating with certified standards procured from Millipore-Sigma and High-Purity Standards. The leached residues were collected from reaction slurry after vacuum filtration on a quantitative (1 µm retention) filter paper and left for overnight drying at 100 °C. Loss on ignition (LOI)(ASTM Standard D7348-13, 2013) was measured as weight loss of ash in a thermogravimetric analyzer (TGA) at 10 °C/min ramp to 950 °C in the zero-air environment.

## 2.3 Geochemical modeling

A geochemical model was built using the PHREEQC v3 program (Parkhurst and Appelo, 2013) with the *wateq4f* thermodynamic database (Ball and Nordstrom, 1991) distributed with PHREEQC. Additional thermodynamic data incorporated into the model, which includes S(IV) speciation and solubility product of CaSO<sub>3</sub>.0.5H<sub>2</sub>O, are provided in Appendix A.2. The program estimates the activity coefficients using extended Debye-Hückel equation from WATEQ (Truesdell and Jones, 1974); wherever the Debye-Hückel activity coefficient parameters are not available, it uses Davies equation (Parkhurst and Appelo, 2013). The model was used to determine the solubility controlling mineral phases, and transport of elements due to washing. The model results are compared with the experimental data. Stoichiometric acid moles and water requirements determined from the titration and batch dissolution experiments were used to simulate acid dissolution requirements to meet ASTM C618 standard (5% SO<sub>3</sub>) under the CO<sub>2</sub> environment and compared with experimental results.

### 3 Results and Discussion

### 3.1 Ash characterization

The chemical oxide and elemental composition of raw SDA ash, as determined by XRF, is shown in Table A.1, and mineral phase identification from the XRD pattern is shown in Figure A.2 (See section A.3 in Appendix provided as e-component). The chemical composition suggests

high-sulfur content (10.44 wt.% as SO<sub>3</sub>), which makes it non-compliant with the ASTM C618 standard, wherein maximum sulfur content allowed is 5.0% (as SO<sub>3</sub> wt.%). Sulfur is mainly in the form of calcium sulfite hemihydrate (CaSO<sub>3</sub>.0.5H<sub>2</sub>O; see dominant peak at 28.3° (2θ) and the phase is represented with open diamonds in Figure A.2). CaO content in the ash is ~26 wt.%, which makes it potentially suitable as a Class C fly ash (ASTM C618 prescribes a minimum of 18.0 wt.%). About 30% of the total calcium in the ash is estimated to be part of the sulfur-rich phase based on the assumption that the sulfur exists only as calcium sulfite hemihydrate. Although calcium sulfates (CaSO<sub>4</sub>) were not detected in the XRD pattern, traces of anhydrite (CaSO<sub>4</sub>) or gypsum (CaSO<sub>4</sub>.2H<sub>2</sub>O) could be present in the ash due to oxidation by exposure to the atmosphere. Other Ca-rich mineral phases include tricalcium aluminate (3CaO.Al<sub>2</sub>O<sub>3</sub> referred to as C<sub>3</sub>A; see dominant peak at 33.2 (20) and the phase represented with down-pointing triangle) and glassy calcium aluminosilicates in addition to unspent portlandite (Ca(OH)<sub>2</sub>) in spray dryer absorber and traces of calcium carbonate (CaCO<sub>3</sub>). A significant fraction of the residue is expected to be made up of fly ash contributing to high SiO<sub>2</sub> (31.8 wt.%) and Al<sub>2</sub>O<sub>3</sub> (15.6 wt.%) content.

Generally, sulfur-rich phases are known to be deposited on the surface of ash particles in Ca-rich fly ashes (Bosbach and Enders, 1998; Izquierdo and Querol, 2012). A study (Taerakul et al., 2005) on surface analysis of spray dry ash reported that the calcium sulfite phase is typically deposited onto the surface of spherical fly ash particles. In addition, considering the relatively slow dissolution rate and low solubility of mineral phases associated with fly ash, i.e., vis-à-vis alkaline-sulfur compounds, selective sulfur extraction is possible.

183

184

185

186

187

188

189

190

191

192

193

194

195

196

197

198

199

200

201

202

#### 3.2 Sulfur extraction characteristics in DI water and the effect of L/S

205 Batch dissolution experiments for sulfur removal from ash were performed in de-ionized (DI) 206 water, and temporal evolution of concentrations of major elements such as Ca, S, Al, Fe, Si, and 207 Mg in the leachate were measured using ICP-OES. Based on the sulfur concentration in the 208 leachate compared to other elements, phenomenological insights into the preferential dissolution 209 of sulfite can be deduced. Figure 1(A) and 2(B) show the concentration of sulfur and the molar 210 ratio of sulfur to calcium versus reaction time, respectively. The molar ratio of S to Ca in the leachate, referred to as S extraction selectivity ( $\hat{S} = [S]/[Ca]$ ), demonstrates the relative extents 211 212 of dissolution of calcium sulfite hemihydrate and other Ca-rich phases in the ash. S concentration 213 in the aqueous phase increased rapidly over the initial five minutes and then plateaued after times 214 greater than 5 minutes, indicative of the system reaching dissolution equilibrium. As shown in Figure 1(B), the initial S extraction selectivity (\$\hat{S}\$) measured after 2 minutes is as high as 0.8 at 215 L/S of 2000 cm<sup>3</sup>/g even though the bulk Ŝ in the raw ash was 0.3. Apart from the sulfite phase, 216 217 Ca from traces of portlandite and calcite from raw ash was assumed to have rapidly leached into 218 the solution. Additionally, the decreasing S selectivity with dissolution time indicates that the 219 relative release of sulfur was found to decrease with time; correspondingly, it may be asserted 220 that the relative losses of Ca from other Ca-rich phases into leachate is higher with the 221 progression of time. The decrease in S selectivity with time is due to decreasing sulfite 222 dissolution rate as the solution approaches equilibrium with respect to CaSO<sub>3</sub>.0.5H<sub>2</sub>O with time. 223 Furthermore, such behavior is anticipated due to decreasing sulfur concentration on the surface 224 of ash particles (as described in Section 3.1) with time because of preferential leaching until the 225 solution is saturated. Since SDA is a combination of fly ash and desulfurization products with S 226 concentrated on the surface of the particles, dissolution for short time durations (e.g., less than 5

minutes) can be used to selectively remove S while retaining other phases associated with the fly ash fraction. Thus, further parametric studies on sulfur dissolution characteristics were conducted using dissolution times of five minutes.

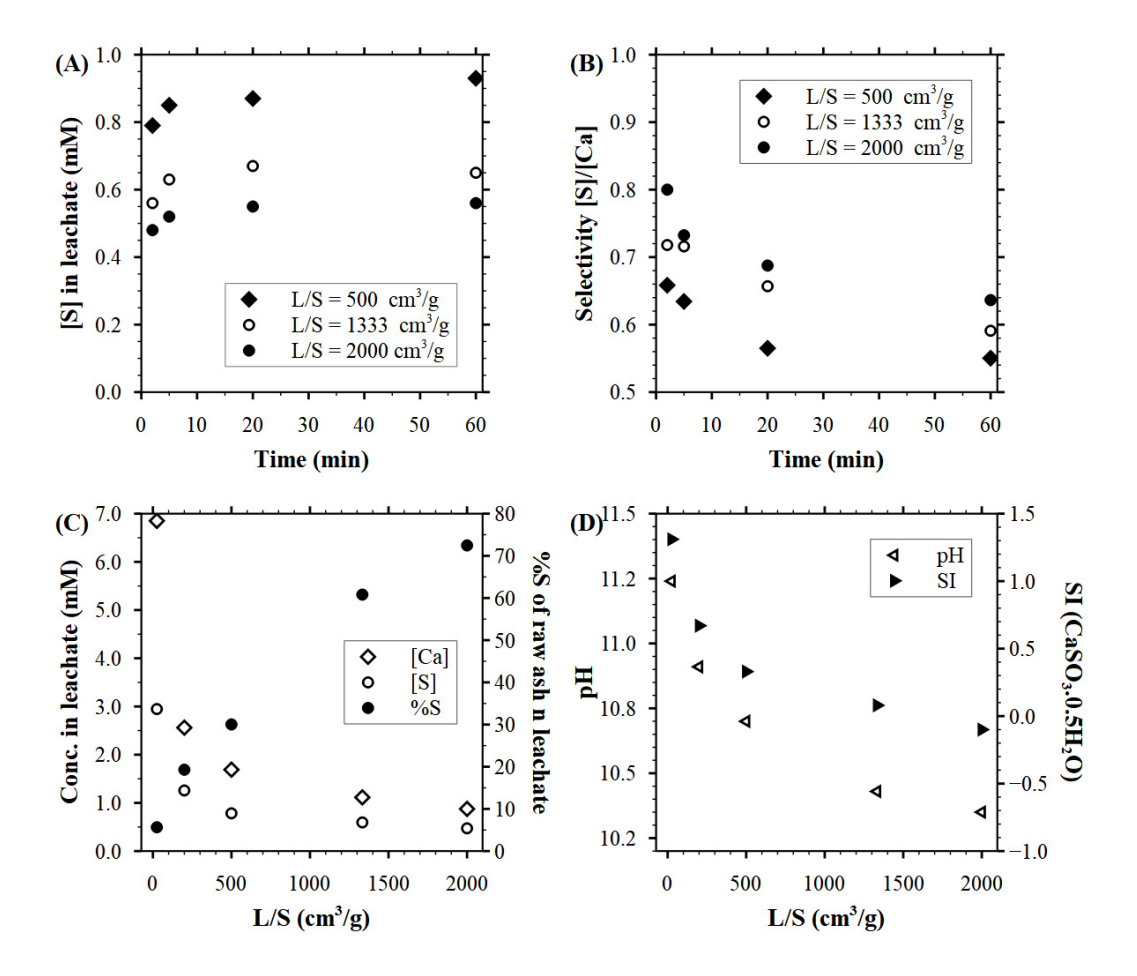


Figure 1 (A) Time-dependent sulfur release from SDA ash into DI water from batch experiments at various liquid-to-solid ratios; (B) corresponding selectivity as a molar ratio of S and Ca in leachate. (C) Effect of L/S on Ca and S concentrations in the leachate and %S extracted from ash after initial five minutes of dissolution; (D) corresponding slurry pH and saturation index (SI) for calcium sulfite hemihydrate phase.

The concentrations of various elements in the leachate released within the first five minutes of the batch dissolution experiment at different liquid-to-solid ratios (L/S) are shown in

Table 1 with Ca and S as the main elements in the leachate. From Figure 1(C), it is clear that the effect of changing L/S impacts leaching of Ca to a greater extent than S, leading to an increase in the S selectivity with increasing L/S (Figure 2(B)). This behavior can be attributed to two factors, firstly, rapid and complete dissolution of Ca-rich minor phases such as portlandite (Ca(OH)<sub>2</sub>) and calcite (CaCO<sub>3</sub>) even at low L/S. Consequently, there is a suppression of calcium sulfite dissolution at low L/S, and no additional Ca contribution from these trace phases at higher L/S. Secondly, the relative dissolution of CaSO<sub>3</sub> at higher L/S is expected to be better than that of kinetically controlled C<sub>3</sub>A, which are sparingly soluble and not as significantly affected by the change in L/S. The supersaturation of calcium sulfite phase in the aqueous phase, shown in Figure 1(D), corroborates its rapid release to approach its solubility limit even at high L/S While the reasons for high supersaturation with respect to calcium sulfite hemihydrate at low L/S are not clear, apart from any inconsistencies between the activity coefficient model and solubility product data, the presence of minor amounts of more soluble S(VI) could be one of the reasons. The concentrations of other elements in the leachate, which were used to calculate saturation indices using PHREEQC, are given in Table 1. Furthermore, the concentration of Al in the leachate, which is expected to be controlled by the solubility of secondary precipitation of gibbsite (Garavaglia and Caramuscio, 1994; Komonweeraket et al., 2015), was found to decrease at lower leachate pH. Thus, it appears that high L/S and more acidic conditions favor the selective S extraction process.

The residual mass and composition of the leached ash were estimated from the mass of elements extracted in solution and are shown in Figure 2(A). The water requirement for decreasing the SO<sub>3</sub> below 5.0 wt.% in the washed ash is estimated to be 1300 cm<sup>3</sup>/g of ash. The corresponding S selectivity in leachate using this amount of water is as high as 0.72 (Table 1),

238

239

240

241

242

243

244

245

246

247

248

249

250

251

252

253

254

255

256

257

258

259

- and the ash weight loss due to washing is estimated to be about 15 wt.% Figure 2(A), thereby 85
- 262 wt.% of the SDA ash is retained for further utilization. As shown in

Table 2, the washed ash composition is compliant with the ASTM C618 standard. The treated residue retained >18 wt% of CaO with >50 wt.% of silica, alumina and iron oxide. However, the high-water intensity may make the washing process impractical. Since acidic conditions (pH  $\sim$  4) result from CO<sub>2</sub>-saturated water solutions produced during aqueous carbonation, further studies were conducted to probe the feasibility of mild acidification to enhance S extraction.

Table 1 Effect of L/S (cm³/g) on concentration (mmol/dm³) of major elements released from W4-SDA into de-ionized water at 23±2 °C.

L/S	Ca	Si	Mg	Al	Na	K	S	[S]/[Ca]	pН	$SI_{Hh}$
25	5.47	0.024	0.011	1.53	0.27	0.098	2.95	0.54	11.24	1.31
200	2.04	0.043	0.024	0.35	0.11	0.006	1.26	0.62	10.91	0.67
500	1.34	0.028	0.015	0.17	0.09	0.004	0.85	0.63	10.70	0.33
1333	0.88	0.019	0.007	0.07	0.07	0.002	0.63	0.72	10.43	0.08
2000	0.70	0.016	0.005	0.05	0.07	0.003	0.52	0.74	10.35	-0.1

Fe concentration in the leachate is lower than the detection limit (0.1 mg/dm<sup>3</sup>) of ICP-OES

SI<sub>Hh</sub> is the saturation index of calcium sulfite hemihydrate defined as the logarithm of the ratio of ionic activity product and solubility product and estimated using PHREEQC.

	Raw	100% S	DI	Acid	Sat. CO <sub>2</sub>	ASTM
Element/phase	Ash	removal <sup>‡</sup>	Water	washing	washing	C618
		estimate		Experimer	ıtal	Standard
CaO	25.9	22.8	22.6	21.7	23.1	≥18.0
$SO_3$	10.4	0	4.3	5.0	4.9	≤5.0
$SiO_2 + Al_2O_3 + Fe_2O_3$	52.3	64.1	60.3	60.7	60.2	≥50.0
Loss on ignition (LOI)†	2.7	-	2.0	1.9	1.4	≤6.0
	1		1			I

<sup>&</sup>lt;sup>‡</sup> For an elementary estimate, it is assumed that all S is present as CaSO<sub>3</sub>, and its leaching is 100% selective.

†LOI is the wt.% loss when the ash sample is heated to 950 °C under zero air environment in a TGA.

#### 3.3 Sulfur extraction characteristics in acid media

Sulfur extraction in mineral acids is expected to proceed via following reaction (e.g. nitric acid),

282 
$$CaSO_3.0.5H_2O(s) + HNO_3(aq) \rightarrow Ca^{+2} + HSO_3^- + NO_3^- + 0.5H_2O.$$

Acid titration using 1.0 N HNO<sub>3</sub> was carried out on an ash slurry at L/S of 25 cm<sup>3</sup>/g to determine the acid requirement to extract the maximum amount of S without decreasing S selectivity (from dissolution of other phases). Figure 2(B) shows the effect of acidification on the extent of sulfur removal and the corresponding S selectivity. Until the point of maximum sulfur removal, the S selectivity increases with acid addition demonstrating preferential and rapid dissolution of calcium sulfite hemihydrate phase vis-à-vis other Ca-rich phases under acidic conditions. The acid requirement for washing to achieve 5.0 wt.% SO<sub>3</sub> in the residue at L/S of 25 cm<sup>3</sup>/g was determined to be 1.43 mmol/g of ash; the corresponding slurry pH was 4.6. The stoichiometric requirement of acid is estimated to be 1.95 meq/mole of S released, and the S selectivity at this ratio is 0.62. As shown in Figure 3, X-ray diffraction confirms substantial reduction and disappearance of peaks corresponding to calcium sulfite hemihydrate (2θ of 16° and 28.3°) after nitric acid extraction with 1.43 mmol/g and 2.0 mmol/g of ash, respectively, while those corresponding to C<sub>3</sub>A (2θ of 33.24°) are retained. As shown in

Table 2, the chemical composition of treated residue from acid-based process to be comparable to that of DI water based process. The combined enrichment of SiO<sub>2</sub>, Al<sub>2</sub>O<sub>3</sub> and Fe<sub>2</sub>O<sub>3</sub> in the treated ash in acidic media (final pH in the range of 4–5) can be associated with their slow dissolution characteristics and poor solubility of hydroxide phases associated with these elements. In an aqueous carbonation process, the acidity can be readily provided by equilibrating the washing solution with gaseous CO<sub>2</sub>. Carbonic acid, as the acidic source, also has the benefit of being recyclable via pressure swing. We, therefore, investigated the sulfur extraction characteristics under different CO<sub>2</sub> partial pressures.



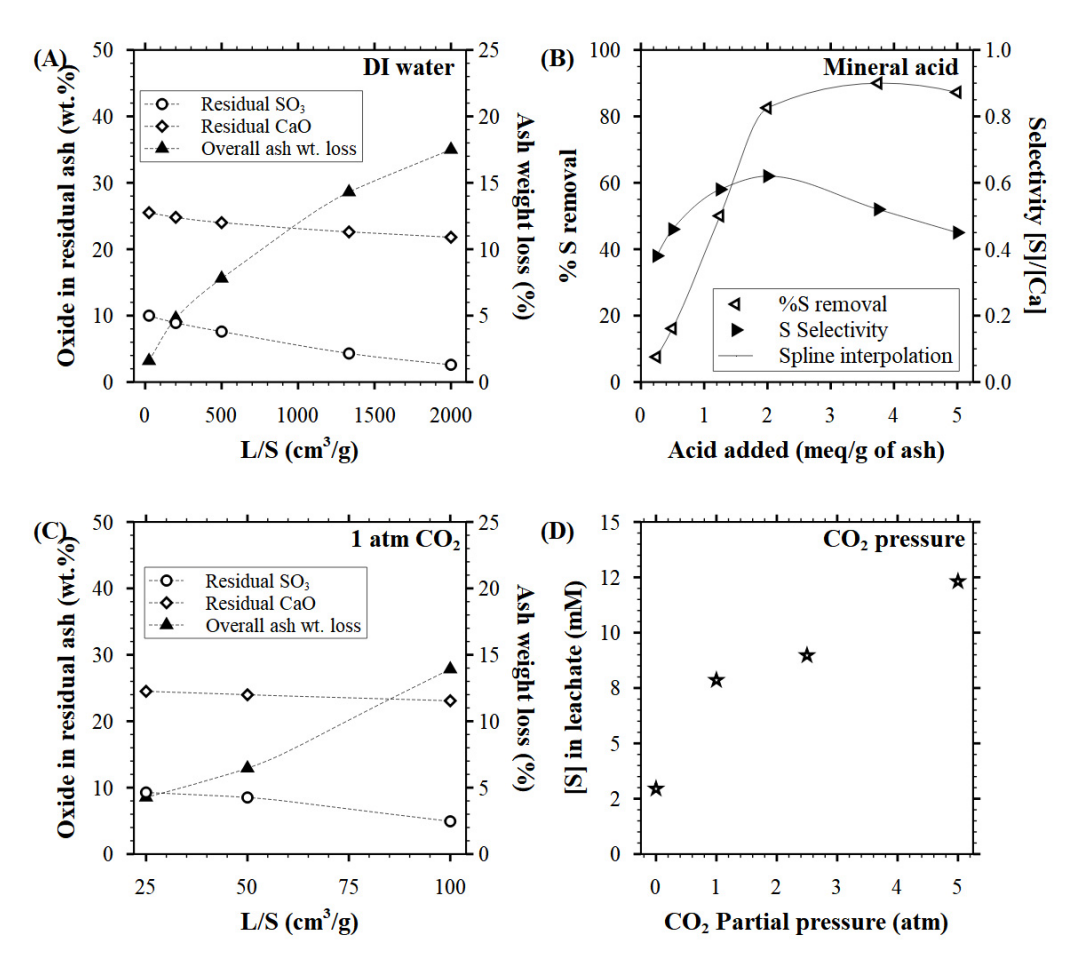


Figure 2 (A) Effect of L/S on chemical oxide composition and weight loss (secondary y-axis) of residual

ash due to washing in DI water, (B) the effect of acid addition on S removal from the ash at L/S of 25 cm<sup>3</sup>/g, (C) Effect of L/S on chemical oxide composition and weight loss (secondary y-axis) of residual ash due to washing in DI water with 1 atm 100% CO<sub>2</sub> pressure, and (D) influence of 100% CO<sub>2</sub> pressure on the solubility of S from W4-SDA; 0 atm represents atmospheric conditions without carbon dioxide input.

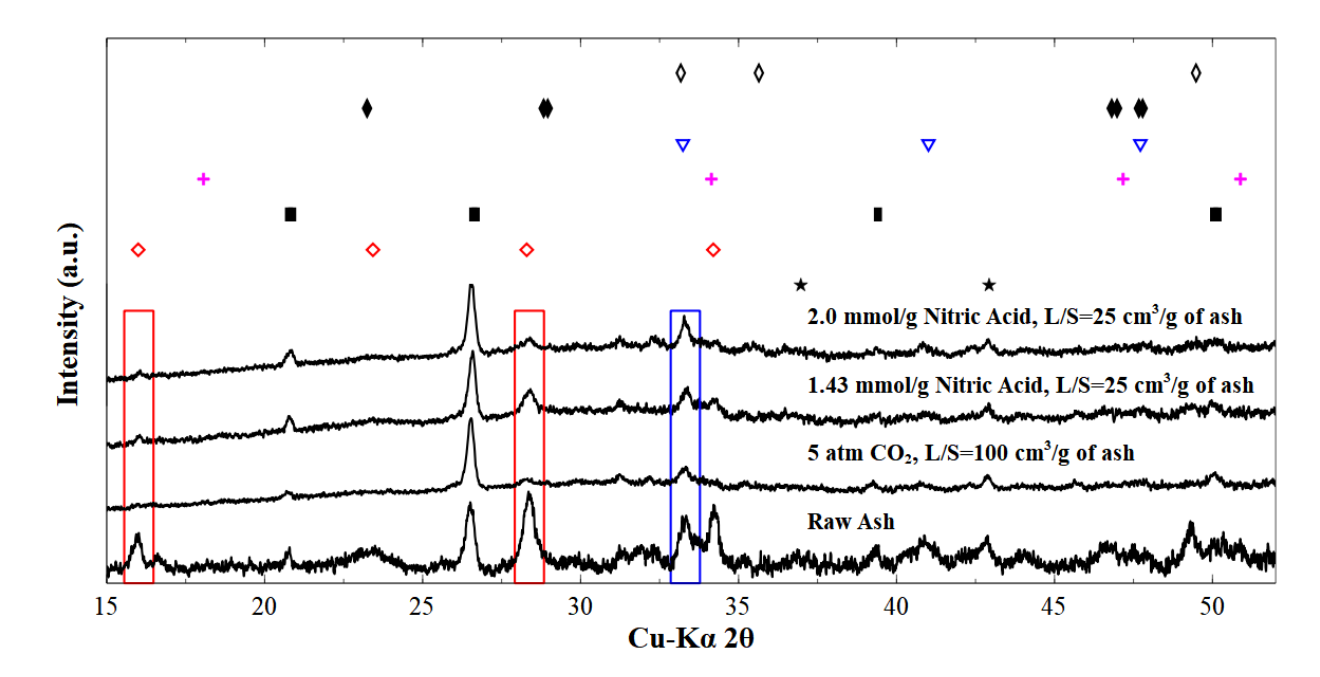


Figure 3 X-ray diffraction pattern of raw W4-SDA ash showing crystalline mineral phases: magnesia (MgO;  $\star$ ), calcium sulfite hemihydrate (CaSO<sub>3</sub>.0.5H<sub>2</sub>O;  $\diamond$ ), quartz (SiO<sub>2</sub>;  $\blacksquare$ ), tricalcium aluminate (3CaO.Al<sub>2</sub>O<sub>3</sub>;  $\triangledown$ ), portlandite (Ca(OH)<sub>2</sub>;  $\clubsuit$ ), calcite (CaCO<sub>3</sub>;  $\diamond$ ), hematite (Fe<sub>2</sub>O<sub>3</sub>;  $\diamond$ ). Changes in calcium sulfite hemihydrate peaks are show using rectangle at 16.0 and 28.3°, and corresponding changes in C3A are shown using rectangle at 33.24° (2 $\theta$ ).

Sulfur extraction in carbonic acid is expected to proceed via following reaction,

$$CaSO_3.0.5H_2O(s) + CO_2(aq) + H_2O \rightarrow Ca^{+2} + HSO_3^- + HCO_3^- + O.5H_2O.$$

The effect of L/S (25–100 cm³/g) and total pressure (1–5 atm) of a 100% CO<sub>2</sub> atmosphere on sulfur extraction characteristics were investigated. The elemental concentrations measured in the leachate and the extent of sulfur removal are shown in Table 3 and Figure 2, respectively. As shown in Figure 2(A) and Figure 2(C), the trends of L/S are similar on residual ash in both DI water and aqueous CO<sub>2</sub> environment, i.e., the same extents of sulfur removal in both the systems

335 resulted in similar chemical composition and weight loss. However, to achieve 5.0 wt.% residual 336 sulfur under a 1 atm CO<sub>2</sub> environment, the L/S was estimated to be 100 cm<sup>3</sup>/g, showing a 337 substantially lower water requirement compared to using DI water (~13 times lower than DI water washing). As shown in Table 3, the concentrations of S in the leachate are similar when 338 L/S was increased from 25 to 100 cm<sup>3</sup>/g under 1 atm CO<sub>2</sub> pressure, which suggests that the 339 release of S into the solution is limited by sulfite solubility. To further improve the S solubility, 340 341 the influence of CO<sub>2</sub> pressure on the release of S was studied (shown in Figure 2(D)). An 342 increase in the CO<sub>2</sub> pressure from 1 atm to 5 atm increased the S solubility by ~57%, showing 343 the potential to reduce the water requirement for sulfur removal to ~50 cm<sup>3</sup>/g. The x-ray 344 diffractogram, shown in Figure 3, shows extent of calcium sulfite removal under 5 atm CO<sub>2</sub> pressure and 100 cm<sup>3</sup>/g to be comparable to residue treated with stoichiometric excess of acid. 345 346 As shown in

Table 2, the treated ash is compliant with ASTM C618 and the chemical characteristics are similar to that obtained from DI water and mineral acid based processes.

Table 3 Effect of L/S (cm³/g) and CO<sub>2</sub> pressure on concentration (mmol/dm³) of major elements released from W4-SDA into the leachate at 23±2 °C.

L/S	Ca	Si	Mg	Al	Na	K	S	[S]/[Ca]	pΗ <sup>†</sup>	SI <sub>Hh</sub>
100%	100% CO <sub>2</sub> – 1 atm abs. pressure									
25	17.04	0.67	1.44	0.017	0.60	0.29	7.88	0.46	5.36	0.46
50	12.51	0.45	1.31	0.023	0.41	0.27	6.24	0.50	5.66	0.55
100	10.76	0.34	2.69	0.227	0.54	0.26	7.75	0.72	5.83	0.73
100% CO <sub>2</sub> – 2.5 atm abs. pressure										
25	19.26	0.72	1.41	0.053	0.92	0.52	8.99	0.47	5.22	0.42
100% CO <sub>2</sub> – 5 atm abs. pressure										
25	23.07	0.96	1.83	0.094	0.95	0.53	12.37	0.54	5.12	0.50

Fe concentration in the leachate is lower than the detection limit (0.1 mg/dm<sup>3</sup>) of ICP-OES

<sup>†</sup>pH for samples under the CO<sub>2</sub> environment was estimated using PHREEQC assuming CO<sub>2</sub> saturation and are not experimentally measured values.

 $SI_{Hh}$  is the saturation index defined as the logarithm of the ratio of ionic activity product and solubility product and estimated using PHREEQC.

### 3.4 Process scheme for sulfur-washing

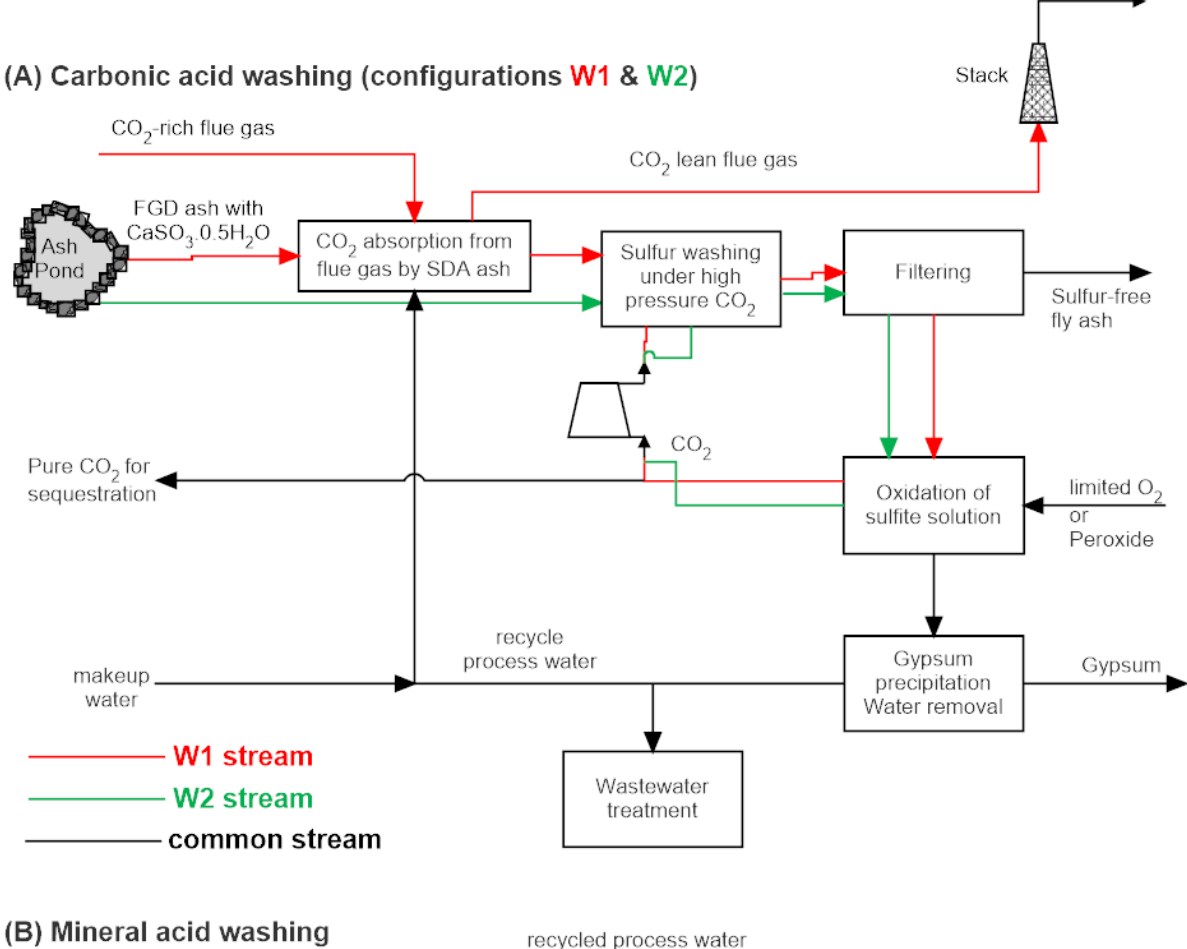
The sulfur dissolution characteristics suggest that selective sulfur removal from SDA ashes may be feasible via weak acid dissolution. In particular, utilizing CO<sub>2</sub> as a recyclable acidic source (i.e., CO<sub>2</sub> saturated solutions) would allow such a process to be integrated into CO<sub>2</sub> mineralization-based carbon capture and utilization processes to reduce potential sulfur contamination in the final products. As such, we propose a combined process of sulfur removal and carbon dioxide capture illustrated in Figure 4. This process is a two-stage absorption-

washing process, where the first stage involves the absorption of carbon dioxide from flue gas into FGD ash slurry to partially dissolve sulfite phase and other rapidly leaching phases in trace quantities. In the following stage, sulfur leaching is carried out using pressurized carbon dioxide (up to 5 atm) to overcome the low solubility of calcium sulfite hemihydrate in aqueous solution. The residual fly ash is filtered at this stage and ready for further processing. The ash residual now has low sulfur content, which can be directly used as SCM or by CO<sub>2</sub> mineralization processes designed for Class C/F fly ash.

The sulfur-rich aqueous stream will be oxidized by the limited supply of O<sub>2</sub> with peroxide addition, which acidifies the solution due to S(IV) oxidation to S(VI) and leads to spontaneous desorption of carbon dioxide (see section A.4 in Appendix). A portion of the desorbed carbon dioxide is compressed and recycled to the sulfur removal step, and the rest is available for CO<sub>2</sub> sequestration or utilization. Sulfate solution, also rich in calcium, may be concentrated either by evaporating or recycling for subsequent precipitation as gypsum; if required, calcium hydroxide may be added at this stage to maximize gypsum precipitation. The process water recovered is recycled to a CO<sub>2</sub> absorber in the first step or sent to wastewater treatment. The pH of the oxidized liquid stream is estimated to be in the range of 3–4, and its recycling is expected to lower the water requirement compared to a single pass system studied here. While the presence of sulfate ions was previously shown to reduce the rate of dissolution of sulfite marginally, by about 10% (Tseng and Rochelle, 1986), we anticipate that such an effect will not be noticeable as sulfite dissolution from the SDA ash appears to be rapid and controlled by its solubility.

A variant of the proposed ash washing process without the carbon capture component is also developed based on mineral acid, e.g., sulfuric acid as the acid source, as shown in Figure 4(B). This process variant can be used to reduce the sulfur content from SDA ashes and make

them potentially usable as SCM for concrete production. As discussed earlier in section 3.3, the acid requirement at L/S of 25 cm<sup>3</sup>/g without recycling of washing solution is estimated to be 1.95 meq/mmol of S(IV) washed. Considering the acid generation due to oxidation of S(IV) to S(VI) and further lowering of pH due to gypsum precipitation, based on the preliminary process simulation studies, the net acid requirement with the recycling of washing solution is expected to be 50% less. As such, net water requirement and effective water circulation for the mineral acid washing process is expected to be much less than that of the CO<sub>2</sub> based process due to lower pH of the solution, and consequently higher solubility of calcium sulfite. Water losses are only expected due to necessary purging such that the accumulation of elements such as chloride ions within the recycle loop is avoided.



(B) Mineral acid washing

recycled process water

To wastewater treatment

FGD ash with

CaSO<sub>3</sub>.0.5H<sub>2</sub>O

Sulfur washing

Oxidation of sulfite solution

Sulfur washing

Figure 4 Block diagram for (A) simultaneous sulfur removal and carbon dioxide capture process; CO<sub>2</sub> capture loop for two different configurations, W1 and W2, are shown in colored lines, (B) acid washing using mineral acids such as sulfuric acid.

## 3.5 CO<sub>2</sub> capture capacity from flue gas

Based on the description of the first stage in the proposed process (see Figure 4(A)), the carbon dioxide capture capacity from flue gas into W4-SDA is the total CO<sub>2</sub> absorbed into the

slurry and includes contributions from physical absorption, and chemically bound bicarbonate and carbonate ions. Here, the contribution of carbonate and bicarbonate ions towards capture capacity is also considered as they are expected to desorb as CO<sub>2</sub> due to acidification of aqueous solution during sulfite oxidation to sulfate by the action of peroxide.

In this study, due to limitations of apparatus, CO<sub>2</sub> capture capacity at simulated flue gas conditions could not be experimentally determined. Alternatively, it was simulated based on the absorbed CO<sub>2</sub> and alkalinity of the leachate, defined as the molar equivalents of bicarbonate ion concentration in the leachate. While the contribution of physically absorbed CO<sub>2</sub> is estimated using Henry's law, the estimation of alkalinity requires the experimental knowledge of all the cations and anions in the solution. However, a conservative estimate of alkalinity can be obtained based on the solubility of CaSO<sub>3</sub>.0.5H<sub>2</sub>O phase by neglecting the calcium release from other phases. As shown in the below balanced chemical reaction, the concentration of bicarbonate ions in the solution would be equal to that of sulfite ions extracted.

$$CaSO_3O.5H_2O + H_2CO_3 \rightarrow Ca^{+2} + HSO_3^- + HCO_3^- + 0.5H_2O$$

It was observed that the predictions for sulfite solubility based on the available thermodynamic data (pK<sub>sp</sub> = 6.574) underestimate the dissolved S concentration from the W4 ash; consequently, saturation indices are positive, suggesting supersaturation (see Table 3). The mismatch in experimental and simulated solubility data may have origins in physical aspects such as temperature difference, or mathematical in nature, where the activity coefficient equation used in the model is inconsistent with the solubility data. The corrected solubility product (as  $pK_{sp}$ ) of calcium sulfite hemihydrate phase was 6.10, which shows saturation of W4-SDA leachate with respect to calcium sulfite hemihydrate phase under 1 to 5 atm of 100% CO<sub>2</sub>

environment (see Appendix A.5) and consequently, appears to be consistent with the used thermodynamic database.

Based on the corrected solubility curve, the sulfur release into aqueous solution saturated with typical coal-fired power plant flue gas (12 vol% CO<sub>2</sub>) at L/S of 50 cm<sup>3</sup>/g is estimated to be 3.79 mM; corresponding absorbed CO<sub>2</sub>, and bicarbonate ion concentrations are 4.07 and 3.79 mM, respectively. The corresponding CO<sub>2</sub> capture potential is estimated to be 17.3 kg/tonne of ash. Since the total dissolved inorganic carbon is only 7.86 mM, any significant CO<sub>2</sub> capture per tonne of ash is possible only at higher L/S values. However, this may not always be desirable due to higher circulation rates and water losses, whose estimation is discussed in the subsequent section.

## 3.6 Critical analysis of process water intensity

A preliminary analysis was carried out to critically examine the water requirement for the proposed process vis-à-vis wet FGD technology commissioned in a 500 MWe supercritical power plant. Here, we attempt this comparison only to understand the water intensity with a known benchmark (wet FGD process) and not to determine if the combination of dry FGD and washing process can be an alternative to the wet FGD process. The design basis for wet FGD technology is based on the work by the U.S. Department of Energy (DOE) for a typical supercritical powerplant (Klett et al., 2007). For comparison, we have used the same design parameters given in the DOE study for the ash washing process, although the SO<sub>3</sub> content of ash in the DOE study is around 44.8 wt.%, which is ~330% higher than the ash used in this study. We do not foresee that the washing process is feasible for such high sulfur ashes, at least using the CO<sub>2</sub> method proposed in this study due to the need for a very high L/S ratio and, consequently, high-water circulation rates. However, water losses can be compared as they

originate mainly due to the carryover by flue gases in the absorber unit and gypsum dewatering unit.

450 Table 4 Comparison of water intensity for Wet FGD and SDA followed by sulfur removal

Process parameter	Units	Value		
A. Power plant design basis				
Net power generation	MW	500		
Net Plant efficiency	%	39.9		
Coal	tonne/day	3877.5		
S in coal	wt.% of coal	4.35		
Fly ash produced	wt.% of coal	8.2		
B. FGD		Wet FGD	<b>SDA</b> + <b>W</b> 1 <sup>‡</sup>	SDA +W2 <sup>‡</sup>
Fly ash	tonne/day	316.8	1139 <sup>\$</sup>	1139 <sup>\$</sup>
%SO <sub>3</sub> in ash*	wt.%	-	44.8	44.8
Dry gypsum produced	tonne/day	1097	0	0
Water Intensity	L/MWhr	220	140	140
C. Washing Process		-	<b>W</b> 1	W2
Liquid-to-solid ratio	cm <sup>3</sup> /g	-	437	437
CO <sub>2</sub> capture	tonne/day	-	170.9	0
Water losses	tonne/day	-	426	318
Water intensity	L/MWhr	-	35.5	26.5
Dry Gypsum produced	tonne/day	-	1059	1059
D. Overall				
Marketable ASTM C618 compliant ash	tonne/day	316.8	344.6	344.6
Water Intensity	L/MWhr	220	175.5	166.5

<sup>451 &</sup>lt;sup>‡</sup>W1, W2 are two- and single-stage washing scenarios, respectively, as described in Section 3.6.

\*SO<sub>3</sub> content in the ash is much higher compared to the ash used in this study. While the washing process may not be ideal for washing such high sulfur ashes, we intend to estimate and compare water intensity with the wet FGD process.

\$ sulfur is assumed to be present as calcium sulfite hemihydrate.

452

453

454

455

456

457

458

459

460

461

462

463

464

465

466

467

468

469

470

471

472

473

Two configurations (W1 and W2) for the proposed carbonic acid based sulfur-washing process shown in Figure 4(A) were examined – i) W1 - both stage 1 and stage 2 for carbon dioxide capture and washing as described in Figure 4, and iii) W2 - only stage 2 for sulfur removal without carbon dioxide capture. A comparison of process parameters for wet FGD and sulfur removal processes are shown in Table 4. The washing process produces similar quantities of gypsum as wet FGD in addition to CO<sub>2</sub> capture of 159 tonnes/day. The water losses in wet FGD are found to be higher than the two-stage washing process, W1, which in turn is higher than the single-stage process without CO<sub>2</sub> capture, W2. Low water intensity for W1 is due to lower flue gas flow rates (~4.6% of total generated) into the absorption column compared to wet FGD process where entire flue gas stream is contacted with process water; in the case without CO<sub>2</sub> capture, W2, water losses are not expected during absorption stage. A marginal contribution in lowering water intensity for washing processes is due to retention of 5.0 wt.% SO<sub>3</sub> in the washed ash. Overall, low water intensity suggests that the sulfur removal process by CO<sub>2</sub> absorptiondesorption is feasible. As such, further experimental studies on CO<sub>2</sub> absorption into ash slurries with recycled process water are needed to understand the accumulation of chloride ions, total dissolved solids, and heavy metal to estimate the recycle to purge ratio of process water. Based on the findings, energy costs associated with water circulation and gypsum precipitation can be estimated for rigorous techno-economic assessment and life cycle assessment.

## 4 Conclusion

The current study is a proof-of-concept for the beneficiation of sulfur-rich coal ashes from dry FGD units in coal-fired power plants by contacting them using recyclable carbonic acid. The process can be integrated with the carbon dioxide mineralization process for value-added products. An alternative scheme using sulfuric acid is also proposed for meeting ASTM C618 compliance without CO<sub>2</sub> capture.

The sulfur extraction from SDA ash is rapid in both alkaline and acidic conditions, as observed in de-ionized water and carbonic acid, respectively. The release of sulfur appears to be limited by the solubility calcium sulfite hemihydrate. The selectivity of sulfur removal was found to be better at low residence time, high liquid-to-solid ratio, and high acidity of the aqueous medium, whereby calcium losses from other mineral phases can be avoided during the washing process. Further, the lower solubility of Al, Fe, and Si in the mildly acidic conditions (pH within the range of 4–6) reduces the washing losses in mineral acid or carbonic acid and shows potential for recovery of high-purity gypsum by oxidation of the leachate. The gravimetric losses due to washing are estimated to be 15 wt.% for the W4-SDA ash, thereby 85 wt.% of the residual ash can be beneficially used as supplementary cementitious material or as feedstock for carbon dioxide mineralization.

Since the process equipment required for the proposed process schemes in this study are similar to existing wet FGD and incinerator ash washing processes, we believe it can be commercialized on a large scale. Key challenges include the recycling of process water and its treatment, and further studies on process simulation and optimization are necessary to identify optimal process parameters and techno-economic assessment.

## Acknowledgment

We thank the WEC Energy Group for providing the SDA ash sample used in this study. This material is based upon work supported by the Department of Energy under Award Number DE-FE0031705. Disclaimer: "This report was prepared as an account of work sponsored by an agency of the United States Government. Neither the United States Government nor any agency thereof, nor any of their employees, makes any warranty, express or implied, or assumes any legal liability or responsibility for the accuracy, completeness, or usefulness of any information, apparatus, product, or process disclosed, or represents that its use would not infringe privately owned rights. Reference herein to any specific commercial product, process, or service by trade name, trademark, manufacturer, or otherwise does not necessarily constitute or imply its endorsement, recommendation, or favoring by the United States Government or any agency thereof. The views and opinions of authors expressed herein do not necessarily state or reflect those of the United States Government or any agency thereof."

## **Appendix**

An appendix is provided along with this manuscript as an e-component.

## References

- ASTM Standard C618 19, 2010. Standard Specification for Coal Fly Ash and Raw or Calcined
- Natural Pozzolan for Use in Concrete. https://doi.org/10.1520/C0618-19
- ASTM Standard D7348-13, 2013. Standard Test Methods for Loss on Ignition (LOI) of Solid
- Combustion Residues. https://doi.org/10.1520/D7348-13
- Ball, J.W., Nordstrom, D.K., 1991. User's Manual for WATEQ4F, with revised thermodynamic

517 data base and test cases for calculating speciation of major, trace, and redox elements in 518 natural waters. U.S. Geol. Surv. Water-Resources Investig. Rep. 519 Bobicki, E.R., Liu, Q., Xu, Z., Zeng, H., 2012. Carbon capture and storage using alkaline 520 industrial wastes. Prog. Energy Combust. Sci. 38, 302–320. 521 Bosbach, D., Enders, M., 1998. Microtopography of high-calcium fly ash particle surfaces. Adv. 522 Cem. Res. 10, 17–23. https://doi.org/10.1680/adcr.1998.10.1.17 523 Carpenter, A.M., 2012. Low water FGD technologies, IEA Clean Coal Center. 524 Chang, R., Kim, S., Lee, S., Choi, S., Kim, M., Park, Y., 2017. Calcium Carbonate Precipitation 525 for CO<sub>2</sub> Storage and Utilization: A Review of the Carbonate Crystallization and 526 Polymorphism. Front. Energy Res. 5, 1–12. https://doi.org/10.3389/fenrg.2017.00017 527 Cruz, M. de A., Araújo, O. de Q.F., de Medeiros, J.L., de Castro, R. de P.V., Ribeiro, G.T., de 528 Oliveira, V.R., 2017. Impact of solid waste treatment from spray dryer absorber on the 529 levelized cost of energy of a coal-fired power plant. J. Clean. Prod. 164, 1623–1634. 530 https://doi.org/10.1016/j.jclepro.2017.07.061 531 DeVilbiss, J., Ray, S., 2017. Sulfur dioxide emissions from U.S. power plants have fallen faster 532 than coal generation [WWW Document]. EIA. 533 Ebrahimi, S., Picioreanu, C., Kleerebezem, R., Heijnen, J.J., van Loosdrecht, M.C.M., 2003. 534 Rate-based modelling of SO2 absorption into aqueous NaHCO3/Na2CO3 solutions 535 accompanied by the desorption of CO2. Chem. Eng. Sci. 58, 3589–3600.

Eloneva, S., Said, A., Fogelholm, C.-J., Zevenhoven, R., 2012. Preliminary assessment of a

29

https://doi.org/10.1016/S0009-2509(03)00231-8

536

538 method utilizing carbon dioxide and steelmaking slags to produce precipitated calcium 539 carbonate. Appl. Energy 90, 329–334. https://doi.org/10.1016/j.apenergy.2011.05.045 540 Enders, M., 1996. The CaO distribution to mineral phases in a high calcium fly ash from eastern 541 germany. Cem. Concr. Res. 26, 243–251. 542 Fuller, E.C., Crist, R.H., 1941. The rate of oxidation of sulfite ions by oxygen. J. Am. Chem. 543 Soc. 63, 1644–1650. https://doi.org/10.1021/ja01851a041 544 Garavaglia, R., Caramuscio, P., 1994. Coal fly-ash leaching behaviour and solubility controlling 545 solids. Stud. Environ. Sci. 60, 87–102. https://doi.org/10.1016/S0166-1116(08)71450-X 546 Harkness, J.S., Sulkin, B., Vengosh, A., 2016. Evidence for Coal Ash Ponds Leaking in the 547 Southeastern United States. Environ. Sci. Technol. 50, 6583–6592. 548 https://doi.org/10.1021/acs.est.6b01727 549 Hoff, S., DeVilbiss, J., 2016. EIA electricity generator data show power industry response to 550 EPA mercury limits [WWW Document]. 551 Izquierdo, M., Querol, X., 2012. Leaching behaviour of elements from coal combustion fly ash: 552 An overview. Int. J. Coal Geol. 94, 54–66. https://doi.org/10.1016/j.coal.2011.10.006 553 Klett, M.G., Kuehn, N.J., Schoff, R.L., Vaysman, V., White, J.S., 2007. Power Plant Water 554 Usage and Loss Study The United States Department of Energy. 555 https://doi.org/10.13140/RG.2.1.5024.6163 556 Komonweeraket, K., Cetin, B., Aydilek, A.H., Benson, C.H., Edil, T.B., 2015. Effects of pH on 557 the leaching mechanisms of elements from fly ash mixed soils. Fuel 140, 788–802. 558 https://doi.org/10.1016/j.fuel.2014.09.068

- 559 Lackner, K.S., Wendt, C.H., Butt, D.P., Joyce, E.L., Sharp, D.H., 1995. Carbon dioxide disposal 560 in carbonate minerals. Energy 20, 1153–1170. https://doi.org/10.1016/0360-561 5442(95)00071-N 562 Ladwig, K.J., Blythe, G.M., 2017. Flue-gas desulfurization products and other air emissions 563 controls, Coal Combustion Products (CCPs): Characteristics, Utilization and Beneficiation. 564 Elsevier Ltd. https://doi.org/10.1016/B978-0-08-100945-1.00003-4 565 Lim, M., Han, G.C., Ahn, J.W., You, K.S., 2010. Environmental remediation and conversion of 566 carbon dioxide (CO<sub>2</sub>) into useful green products by accelerated carbonation technology. Int. 567 J. Environ. Res. Public Health 7, 203–228. https://doi.org/10.3390/ijerph7010203 568 McCarthy, G.J., Solem, J.K., Manz, O.E., Hassett, D., 1990. Use of a database of chemical, 569 mineralogical and physical properties of north american fly ash to study the nature of fly 570 ash and its utilization as a mineral admixture in concrete. Mat. Res. Soc. Symp. Proc. 178, 571 3–33. https://doi.org/10.1557/PROC-178-3 572 Mehdipour, I., Falzone, G., La Plante, E.C., Simonetti, D., Neithalath, N., Sant, G., 2019. How 573 microstructure and pore moisture affect strength gain in portlandite-enriched composites 574 that mineralize CO<sub>2</sub>. ACS Sustain. Chem. Eng. 7, 13053–13061. 575 https://doi.org/10.1021/acssuschemeng.9b02163 576 Olajire, A. a., 2013. A review of mineral carbonation technology in sequestration of CO<sub>2</sub>. J. Pet. 577 Sci. Eng. 109, 364–392. https://doi.org/10.1016/j.petrol.2013.03.013
- Pan, S.-Y., 2012. CO<sub>2</sub> Capture by Accelerated Carbonation of Alkaline Wastes: A Review on Its
   Principles and Applications. Aerosol Air Qual. Res. 770–791.
- 580 https://doi.org/10.4209/aaqr.2012.06.0149

581 Parkhurst, D.L., Appelo, C.A.J., 2013. Description of input and examples for PHREEQC version 582 3: a computer program for speciation, batch-reaction, one-dimensional transport, and 583 inverse geochemical calculations, Techniques and Methods. Reston, VA. 584 https://doi.org/10.3133/tm6A43 585 POWER, 2008. Wisconsin Public Service Corp.'s Weston 4 earns POWER's highest honor 586 [WWW Document]. POWER Mag. URL https://www.powermag.com/wisconsin-public-587 service-corp-s-weston-4-earns-powers-highest-honor/ (accessed 10.15.20). 588 Ríos, A., González, M., Montes, C., Vásquez, J., Arellano, J., 2020. Assessing the effect of fly 589 ash with a high SO<sub>3</sub> content in hybrid alkaline fly ash pastes (HAFAPs). Constr. Build. 590 Mater. 238, 117776. https://doi.org/10.1016/j.conbuildmat.2019.117776 591 Samad, S., Shah, A., 2017. Role of binary cement including Supplementary Cementitious 592 Material (SCM), in production of environmentally sustainable concrete: A critical review. 593 Int. J. Sustain. Built Environ. 6, 663–674. https://doi.org/10.1016/j.ijsbe.2017.07.003 594 Sarudi, I., Varga-Cseresnyés, E., Csapó-Kiss, Z., Szabó, A., 2001. Elimination of disturbing 595 effect caused by sulphur dioxide for sulphur determination in wines by ICP-OES. Anal. 596 Lett. 34, 449–455. https://doi.org/10.1081/AL-100102586 597 Sharifi, N.P., Jewell, R.B., Duvallet, T., Oberlink, A., Robl, T., Mahboub, K.C., Ladwig, K.J., 2019. The utilization of sulfite-rich Spray Dryer Absorber Material in portland cement 598 599 concrete. Constr. Build. Mater. 213, 306-312. 600 https://doi.org/10.1016/j.conbuildmat.2019.04.074 601 Taerakul, P., Sun, P., Walker, H., Weavers, L., Golightly, D., Butalia, T., 2005. Variability of 602 inorganic and organic constituents in lime spray dryer ash. Fuel 84, 1820–1829.

603	https://doi.org/10.1016/j.fuel.2005.03.015
604	Teir, S., Eloneva, S., Zevenhoven, R., 2005. Production of precipitated calcium carbonate from
605	calcium silicates and carbon dioxide. Energy Convers. Manag. 46, 2954–2979.
606	Truesdell, A.H., Jones, B.F., 1974. WATEQ, a Computer Program for Calculating Chemical
607	Equilibria of Natural Waters. J. Res. U.S. Geol. Surv.
608	Tseng, P.C., Rochelle, G.T., 1986. Dissolution Rate Of Calcium Sulfite. Environ. Prog. 5.
609	Vaziri Hassas, B., Rezaee, M., Pisupati, S. V., 2020. Precipitation of rare earth elements from
610	acid mine drainage by CO2 mineralization process. Chem. Eng. J. 399, 125716.
611	https://doi.org/10.1016/j.cej.2020.125716
612	Wee, J.H., 2013. A review on carbon dioxide capture and storage technology using coal fly ash
613	Appl. Energy 106, 143–151. https://doi.org/10.1016/j.apenergy.2013.01.062
614	Wei, Z., Wang, B., Falzone, G., La Plante, E.C., Okoronkwo, M.U., She, Z., Oey, T., Balonis,
615	M., Neithalath, N., Pilon, L., Sant, G., 2018. Clinkering-free cementation by fly ash
616	carbonation. J. CO2 Util. 23, 117–127. https://doi.org/10.1016/j.jcou.2017.11.005
617	Zaremba, T., Mokrosz, W., Hehlmann, J., Szwalikowska, A., Stapinski, G., 2008. Properties of
618	the Wastes Produced in the semi-dry FGD Installation. J. Therm. Anal. Calorim. 93, 439-
619	443.
620	